



Chloride channel gene expression in the rabbit cornea

Natalie Davies,¹ Saeed Akhtar,¹ Helen C. Turner,² Oscar A. Candia,^{2,3} Chi Ho To,⁴ Jeremy A. Guggenheim¹

¹School of Optometry and Vision Sciences, Cardiff University, Redwood Building, King Edward VII Avenue, Cardiff, UK; Departments of ²Ophthalmology and ³Physiology and Biophysics, Mount Sinai School of Medicine, 100th Street and 5th Avenue, New York, NY; ⁴Department of Optometry & Radiography, Hong Kong Polytechnic University, Hung Hom, Hong Kong

Purpose: The maintenance of stromal hydration by the corneal endothelium relies on active transendothelial anion transport, with bicarbonate and chloride the major anions carrying the current. However, the ion transport pathways that operate to maintain stromal hydration have yet to be fully elucidated.

Methods: We used RT-PCR to identify the gene expression profile of members of the CIC family of chloride channels in freshly isolated samples of rabbit corneal endothelium, stroma, and epithelium. The expression of a separate group of genes was also examined to confirm the purity of the sample collection protocol. The expression of the CIC-2 and CIC-3 channel protein in the cornea was also evaluated by light and electron microscopic immunolabelling.

Results: The mRNA for CIC-2, CIC-3, CIC-5, CIC-6, and CIC-7 were expressed in both the corneal epithelium and endothelium, and in the stroma. The mRNA for the skeletal muscle specific channel CIC-1 and the kidney specific chloride channel CIC-Ka were not detectable. CIC-4 mRNA was not detected in any rabbit tissue examined. The expression pattern of the mRNAs for collagens V, VI, VII, and VIII demonstrated the absence of contamination in epithelial and endothelial samples. CIC-2 and CIC-3 immunolabelling confirmed the presence of these proteins in corneal endothelium, stroma, and epithelium.

Conclusions: Together with cystic fibrosis transmembrane conductance regulator (CFTR) and calcium activated chloride channel-1 (CLCA1), these results bring the number of chloride channel genes known to be expressed in the corneal endothelium and epithelium to seven. These channels are likely to be important for the maintenance of corneal transparency.

The hydration of the corneal stroma is maintained by a balance between its tendency to swell and an active process of ion transport across the corneal endothelium [1]. The tendency to swell is due to the presence in the stromal matrix of non-diffusible, negatively charged molecules such as glycosaminoglycans [2,3]. Ion transport across the endothelium is thought to involve the active transport of anions from the stroma towards the aqueous humor, followed by the mainly passive diffusion of cations [4]. The osmotic effect of this transendothelial ion transport counters the osmotic potential excess of the stroma. At hydrations outside the normal range, the cornea loses its transparency [5]. Thus, defective endothelial ion transport leads to stromal swelling, loss of corneal transparency and impaired vision.

Mutations in the genes encoding ion transport proteins have been found to cause a number of genetic diseases [6,7]. This makes the ion transporters of the cornea attractive candidate genes for certain corneal dystrophies. The pathways by which anions are transported across the corneal endothelium have yet to be fully elucidated. However, Bonanno [4] proposed a new model of corneal endothelial ion transport that explains much of the previously contradictory literature in this area. In the new model, bicarbonate (HCO_3^-) is considered the

major anion that is actively transported [8]. Although it is not known for certain whether chloride is also actively transported across the corneal endothelium [4,9], it is clear that chloride is an essential part of the endothelial pump mechanism [10].

Chloride channels are strongly implicated in corneal endothelial ion transport [11-16]. In this investigation, we focus on the CIC family of voltage gated chloride channels. This gene family comprises nine members in humans, comprising seven widely expressed chloride channels named CIC-1 to CIC-7 along with two kidney specific channels, CIC-Ka and CIC-Kb. The precise function of many of these channels is not yet known, but they have been suggested to mediate Cl^- transport both into and out of the cell, and intracellularly (for example, in organelle volume regulation) [17,18]. We studied the mRNA expression of members of the CIC family in one of the best established animal models of corneal physiology, the rabbit. Part of this work has been presented previously in abstract form [19].

METHODS

Tissue samples and RNA extraction: This work followed the Guiding Principles in the Care and Use of Animals (DHEW Publication, NIH 80-23). Adult male New Zealand White rabbits (2.0-2.5 kg) were killed with an overdose of sodium pentobarbital. Non-ocular tissues (kidney, lung, muscle, and skin) were collected using a fresh sterile disposable scalpel for each, dissected into cubes (side length 3-5 mm), rinsed in sterile phosphate buffered saline, pH 7.4 (PBS), and snap frozen in

Correspondence to: Jeremy A. Guggenheim, School of Optometry & Vision Sciences, Cardiff University, Cardiff, CF10 3NB, Wales, United Kingdom; Phone: +44 (0) 29 2087 5063; FAX: +44 (0) 29 2087 4859; email: guggenheim@cardiff.ac.uk

liquid nitrogen. Eyes were enucleated and the corneas rinsed with sterile PBS. A new blade was used to scrape off corneal epithelial cells from the central cornea, which were shaken into a micro-centrifuge tube containing 1 ml of TriReagent (Sigma-Aldrich Co. Ltd., Poole, United Kingdom). The cornea, with a scleral rim, was then dissected from the globe and laid endothelial side uppermost in a sterile Petri dish. A new blade was used to excise a square of cornea from within the limbal region, and endothelial cells from this square were gently scraped off using another fresh scalpel and shaken into a second tube of TriReagent. The remaining button of stroma was washed in PBS and frozen in liquid nitrogen. All tissues were collected within 30 min of death to minimize RNA degradation.

RNA was extracted as described previously [20]. For solid tissues (all those except corneal epithelium and endothelium), this involved a preliminary homogenization step at liquid nitrogen temperature in a freezer mill (Mikrodismembrator; Braun Biotech Ltd., Melsungen, Germany) in the presence of TriReagent. RNA was then extracted following the manufacturer's protocol, followed by DNase treatment, phenol-chloroform extraction, and ethanol precipitation. RNA was re-suspended in RNase free water, examined by agarose gel electrophoresis and quantified by spectrophotometry (absorbance at 260 nm).

Reverse transcription polymerase chain reaction (RT-PCR): PCR primers were designed for the chloride channels CIC-1 through CIC-7 and for one of the kidney specific CIC (CIC-Ka) mRNAs: This latter channel served as a negative control, since its expression was not expected in the cornea. Mammalian CIC mRNA sequences were downloaded from GenBank and used to generate a series of multiple sequence alignments using CLUSTAL-W [21]. Two types of alignments were generated. First, for each CIC, the available mRNAs (e.g., human, mouse, etc.) were aligned to provide areas of consensus sequence. Second, mixed CIC alignments were generated to identify areas of disparity between the different members

of the gene family. At least partial cDNA sequences for six of the nine known CICs were available for the rabbit. PCR primers were chosen such that they were in a region that matched the consensus sequence for that CIC (and in particular, the rabbit sequence, where this was known) and yet were not in regions where the cDNA sequence was conserved between different members of the gene family. In general, primers were chosen to be about 20 bp in length, with a GC content of 50-60% and no long repeats of a single base. A lack of cross-reactivity between the 3' end of the CIC primers and other known genes was confirmed by BLAST searches. Annealing temperatures were calculated according to a nearest neighbor algorithm [22]. If primers performed poorly in empirical tests then they were redesigned up to four times. The optimized primer sequences used in the study are shown in Table 1.

RNA (1 µg) from each tissue source was denatured at 70 °C for 5 min, cooled to 37 °C and reverse transcribed in a 20 µl reaction containing 1X RT buffer (Invitrogen, Groningen, The Netherlands), 0.5 mM each dNTP, 10 mM dithiothreitol, 40 U RNase-OUT (Life Technologies, Paisley, United Kingdom), and 200 U Superscript II reverse transcriptase (Invitrogen). The reverse transcription reaction was carried out at 37 °C for 30 min followed by 45 °C for 30 min. Excess oligo-dT was removed using a spin-column (Qiaquick, Qiagen, Crawley, United Kingdom) and the cDNA eluted in 50 µl of 10 mM Tris-HCl buffer, pH 8.0. Mock reverse transcriptase reactions that contained all of the reagents above except for the reverse transcriptase enzyme itself were done to ensure that DNA contamination of mRNA samples did not give rise to false positive amplification products. PCR was carried out in 40 µl reaction volumes containing 5 µl of undiluted cDNA, 1X PCR buffer (Promega, Southampton, United Kingdom), 1.5 mM MgCl₂, 0.2 mM each dNTP, 1 µM each primer, and 1 U Taq polymerase (Promega). After 35 cycles of 94 °C for 1 min, annealing temperature (Table 1) for 1 min, and 72 °C for 1 min, the products were evaluated on a 2% agarose gel and

TABLE 1. CIC PCR PRIMERS

Name	Sequence (5'-3')	T _m (°C)	Annealing temperature (°C)	Product size (bp)
C1C-1	F: GTGTATCTGCATCGCCAAG	63	59	712
	R: TGGTATATTTGCTGAGCTGGTT	63		
C1C-2	F: GGGCCTGGTGGAGGAGCT	70	66	238
	R: GAATCCCCTCGGGGAACC	70		
C1C-3	F: GTAGTAACACTAACAGGATTGGC	59	54	419
	R: ACTAATGTGATGGTTTTAATCATT	58		
C1C-4	F: CYTGGTACATGGCTGAACCTCT	60	56	418
	R: GGRATCTTCATGCCAAAGGTA	62		
C1C-5	F: ACACCGATGAGGGAGCGTT	68	63	848
	R: GCTTGTGTGAAACGGTTCTCA	67		
C1C-6	F: GATGGTACGAGTGGTGAAGTGA	71	66	627
	R: AGAAGAGCACTTTCATGTGAGCC	70		
C1C-7	F: GTGGTCTCTTCTGGAACAGTT	70	66	441
	R: TGGAGTTGTACTCGCCATCTGC	70		
C1C-Ka	F: ACCCCCTGGTGGAGAGCA	70	63	385
	R: CTGGACGCCACAGTCACC	67		

Primers were designed and tested as described in the Methods section.

TABLE 2. GENE SPECIFIC PCR PRIMERS

Name	Sequence (5'-3')	T _m (°C)	Annealing temperature (°C)	Product size (bp)
Collagen V	F: GGYTCCTGGTTCAGTGAA	58	53	420
	R: CTCTARCCYATGAAGCAAG	57		
Collagen VI	F: GGATACCAAGGCAACAACGGA	69	63	194
	R: GCTGAGACCTCTCCAGCCA	67		
Collagen VII	F: GGTCTGCATCCTGATCAGAGA	67	63	896
	R: CCTCAGGCACCAAGTTCCA	68		
Collagen VIII	F: CCAGGAGTAGCAGGACTTCA	63	57	471
	R: CTCGTCGTACGTGTACATCA	61		
Connexin 43	F: TTCATCATCTTCATGCTGGT	62	58	368
	R: TGGAGTTAGAGATGGTCT	62		
Decorin	F: CACCATCCCTCAAGTCT	61	57	267
	R: CAGGTTGTCTACCTCATAACAA	61		
Annexin II	F: CCACCTCCAGAAAGT	51	45	306
	R: GCAAGACACTAAGGG	49		
Keratin 12	F: GCCTACATGAAGAAGAACCA	67	63	255
	R: GACCTCGCTCTTGTGACT	67		
NBC	F: GTGCCAAGTGAAGTTCAAGCCA	69	63	753
	R: GACATCATCIAGGAAGCTGAG	61		

Primers were designed and tested as described in the Methods section.

stained with SYBR gold (Molecular Probes, Leiden, The Netherlands). To be considered as “present”, at least two out of three replicate PCR experiments had to show a positive result for a given CIC. Each replicate experiment used cDNA originating from a different eye (or a different piece of tissue, for non-ocular samples).

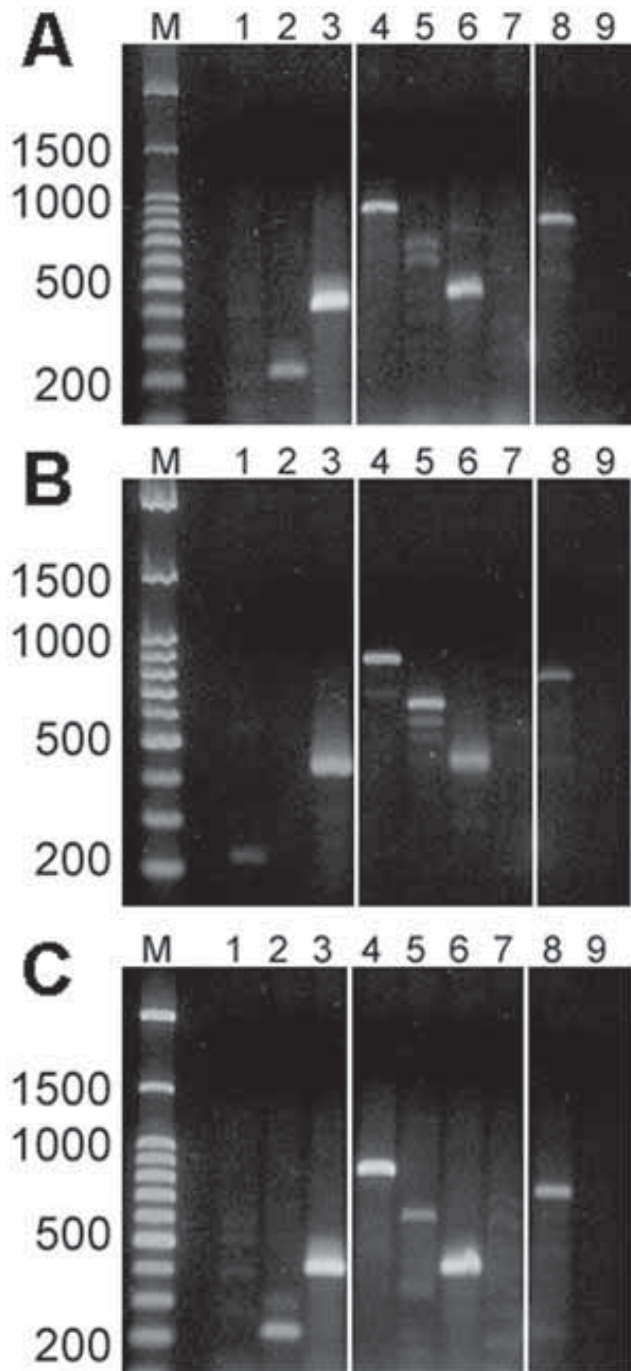


Figure 1. Gel electrophoresis of RT-PCR products for members of the CIC family. **A:** Epithelial cell sample. **B:** Stromal sample. **C:** Endothelial cell sample. Lane M: Molecular weight marker. Lane 1: CIC-1. Lane 2: CIC-2. Lane 3: CIC-3. Lane 4: CIC-5. Lane 5: CIC-6. Lane 6: CIC-7. Lane 7: CIC-Ka. Lane 8: NBC positive control. Lane 9: NBC negative control.

To confirm the identity of PCR products, each was amplified in bulk (5X 40 μ l), pooled, phenol-chloroform extracted, ethanol precipitated, and run on a preparative 2% agarose gel containing 10 μ g/ml of 0.2 μ m-filtered crystal violet (Sigma). The band containing the PCR product, visualized using a Model TM-20 transilluminator (UVPLtd., Cambridge, United Kingdom), was excised using a sterile blade. DNA was eluted from the gel slice using a spin-column procedure (Qiagen), cloned into a T-tailed pBluescript plasmid, and used to transform competent DH5 α E. coli [23]. For each PCR product, miniprep DNA from six recombinant colonies were sequenced on an ABI 3100 sequencer (Cardiff University Molecular Biology Resource Center). Sequence identity was assessed using BLAST database searches at the NCBI against the nonredundant sequence database.

Cell type specific gene expression: A literature search was carried out to identify genes whose expression has been shown to be limited to corneal epithelial cells, corneal endothelial cells, or stromal keratocytes. From this list, keratin 12, and collagens type V, VI, VII, and VIII were chosen as candidate cell type specific genes. The presence of the mRNA for these genes was assessed in corneal tissue samples in order to determine the extent of any cross-contamination in the tissue collection protocol. Connexin 43, annexin II, and decorin were used as positive controls whose expression was expected in all cell layers of the cornea. Sodium bicarbonate cotransporter (NBC) was used as an additional positive control after it too was found to show robust expression in mRNA extracted from each cell layer. For each gene, the design of primers and the PCR reactions themselves were carried out as described above, except that for a preliminary set of triplicate experiments, gels were stained with ethidium bromide instead of SYBR gold. Primer sequences are shown in Table 2. PCR products were sequenced to confirm their identity as described above.

Immunocytochemistry: Affinity purified primary antibodies were obtained from Alomone Labs (Silverstone, United Kingdom). The anti-CIC-2 antibody was raised against residues 888-906 of rat CIC-2 (P35525) and the anti-CIC-3 antibody was raised against residues 592-661 of rat CIC-3 (P51792). Since these antibodies were raised in rabbit, we tested corneal CIC expression in human and rat tissue, where they have been carefully characterized previously [24].

TABLE 3. CIC GENE EXPRESSION IN THE RABBIT CORNEA BY RT-PCR

Gene	Epithelium	Stroma	Endothelium
CIC-1	No	No	No
CIC-2	Yes	Yes	Yes
CIC-3	Yes	Yes	Yes
CIC-4	No	No	No
CIC-5	Yes	Yes	Yes
CIC-6	Yes	Yes	Yes
CIC-7	Yes	Yes	Yes
CIC-Ka	No	No	No

The table shows the results from three replicate experiments (see Methods). Gels were stained with SYBR Gold.

For light microscopy, freshly isolated human corneal segments were positioned in cryomatrix embedding medium and quick frozen in liquid nitrogen. Cryosections (5-10 μm thick) were cut and collected on gelatin coated slides. Consecutive tissue sections were fixed in either ice cold methanol at -20 °C for 10 min or 4% paraformaldehyde at room temperature. Nonspecific binding sites were blocked with PBS containing 2% bovine serum albumin (BSA) plus 0.3% Triton X-100, for 30 min at room temperature. Primary antibodies, diluted 1:100 in 1% BSA-PBS and 0.3% Triton X-100 were applied to corneal sections overnight at 4 °C in a moist chamber. Following several washes in PBS, the tissue sections were labeled with a specific Alexa Fluor-488 conjugated secondary antibody (Molecular Probes) diluted 1:800, for 1 h at room temperature and mounted with Vectashield (Vector Labs, Peterborough, United Kingdom). Fluorescent signals were visualized on a Zeiss Axiophot fluorescent microscope. Competition experiments were carried out by pre-absorbing the isoform specific primary antibody with an excess of the corresponding respective antigen for 3-4 h at 4 °C. This pre-absorption was followed by the standard immunodetection protocol. Human eye tissue was provided by the National Disease Research Interchange

(NDRI, Philadelphia, PA) and used between 24-48 h of death. Donors were between 50-65 years old.

For electron microscopy, pieces of rat cornea were fixed in freshly prepared 4% paraformaldehyde in 0.1 M phosphate buffer (PB) for 2 h at 4 °C. Tissue was washed 3 times for 15 min each in 0.1 M PB and dehydrated in 30%, 50% (4 °C), and 70% to 100% ethanol (-20 °C; 1 h in each). Tissues were infiltrated at -20 °C in two changes (1 h each) of a 1:1 mixture of 100% ethanol and LR White resin (-20 °C) and three changes (8 h each) of LR White only (-20 °C). Tissue blocks were then incubated at -20 °C for 48 h under UV light to polymerize the LR White. Ultrathin sections cut from the blocks were collected on formvar-carbon coated, 200-mesh nickel grids. Three blocks from each region of the cornea were used for immunoelectron microscopy.

Sections were treated at room temperature by floating them on to a 50 μl drop of PBS containing 0.1% bovine serum albumin (PBS-BSA) for 15 min, then PBS-BSA containing 5% normal goat serum for 30 min. They were incubated overnight with primary antibodies (at 1:20) dilution. To remove unbound antibody, sections were washed with 0.05 M Tris buffered saline (TBS), pH 7.4 (three washes, 5 min each), TBS pH 7.4 containing 0.2% BSA (three washes, 5 min each), and TBS, pH 8.4 containing 1% BSA (three washes, 5 min each). Sections were then incubated with 10 nm immunogold conjugated goat anti-rabbit secondary antibodies (Biocell Ltd., UK) diluted 1:25 in TBS, pH 8.4 containing 1% BSA, for 50 min. Unbound secondary antibody was removed by washing in TBS-BSA (three washes, 5 min each), PBS (three washes, 5 min each), and distilled water (three washes, 5 min each). Controls were performed by omitting the primary antibody. Three replicate experiments were carried out for each antibody used. Sections were stained with 2% aqueous uranyl acetate and lead citrate and examined in a JEOL 1010 transmission electron microscope (JEOL Ltd., Akishima, Japan).

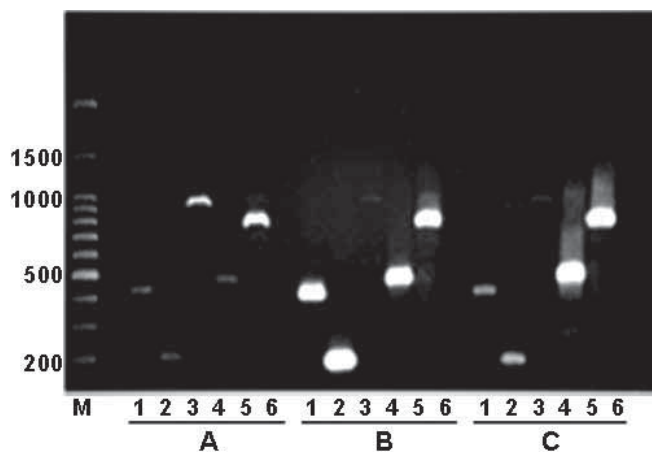


Figure 2. Gel electrophoresis of RT-PCR products for corneal cell type specific genes. Group A: Epithelial cell sample. Group B: Stromal sample. Group C: Endothelial cell sample. Lane M: molecular weight marker. Lane 1: Type V collagen. Lane 2: Type VI collagen. Lane 3: Type VII collagen. Lane 4: Type VIII collagen. Lane 5: NBC positive control. Lane 6: NBC negative control.

RESULTS

CIC Chloride channel gene expression: Sets of PCR primers were designed that would amplify each member of the CIC family in rabbit (Table 1). When tested on tissues with known CIC expression profiles, such as muscle and kidney, these primers gave rise to products of the expected size in the expected tissue types (data not shown). The panel of primers was used to evaluate the CIC gene expression profile of the rabbit cor-

TABLE 4. CELL TYPE SPECIFIC GENE EXPRESSION IN THE RABBIT CORNEA BY RT-PCR

Gene	Ethidium bromide			SYBR Gold		
	Epithelium	Stroma	Endothelium	Epithelium	Stroma	Endothelium
Collagen V	No	Yes	Yes	Yes	Yes	Yes
Collagen VI	No	Yes	Yes	Yes	Yes	Yes
Collagen VII	Yes	No	No	Yes	Yes	No
Collagen VIII	No	Yes	Yes	Yes	Yes	Yes
Keratin 12	Yes	Yes	Yes	Yes	Yes	Yes

The table shows the results from six replicate experiments (see Methods) in which gels were stained with either ethidium bromide or SYBR Gold.

neal epithelium, endothelium and stroma. When a positive RT-PCR result was obtained using corneal mRNA, the PCR product was sequenced to confirm its identity. Where positive PCR products were not produced for the corneal samples, the PCR product generated from an alternative rabbit tissue was sequenced, to validate that the primers did amplify rabbit cDNA effectively. In all but one case, the primers amplified the expected CIC product (as judged by the highest scoring BLAST hit). The exception was CIC-4, as discussed below. The degree of nucleotide identity between the rabbit CIC-1 and CIC-7 PCR products (those for which a rabbit cDNA sequence was not available in the database) and the corresponding regions of their human orthologs was 92% in both cases.

CIC chloride channel mRNAs were found to be widely expressed in each layer of the rabbit cornea (Figure 1, Table 3). Thus, the mRNAs for CIC-2, CIC-3, CIC-5, CIC-6, and CIC-7 were all detected in the corneal epithelium, stroma, and endothelium. By contrast, the skeletal muscle specific CIC-1 mRNA could not be detected in any layer of the cornea, as was also the case for the kidney specific channel, CIC-Ka. Mock reverse transcription reactions, used as a negative control to test for genomic DNA contamination of mRNA samples, were uniformly negative.

Cell type specific gene expression: To confirm that CIC channel gene expression in the different corneal layers was not due to cross-contamination during tissue collection, the

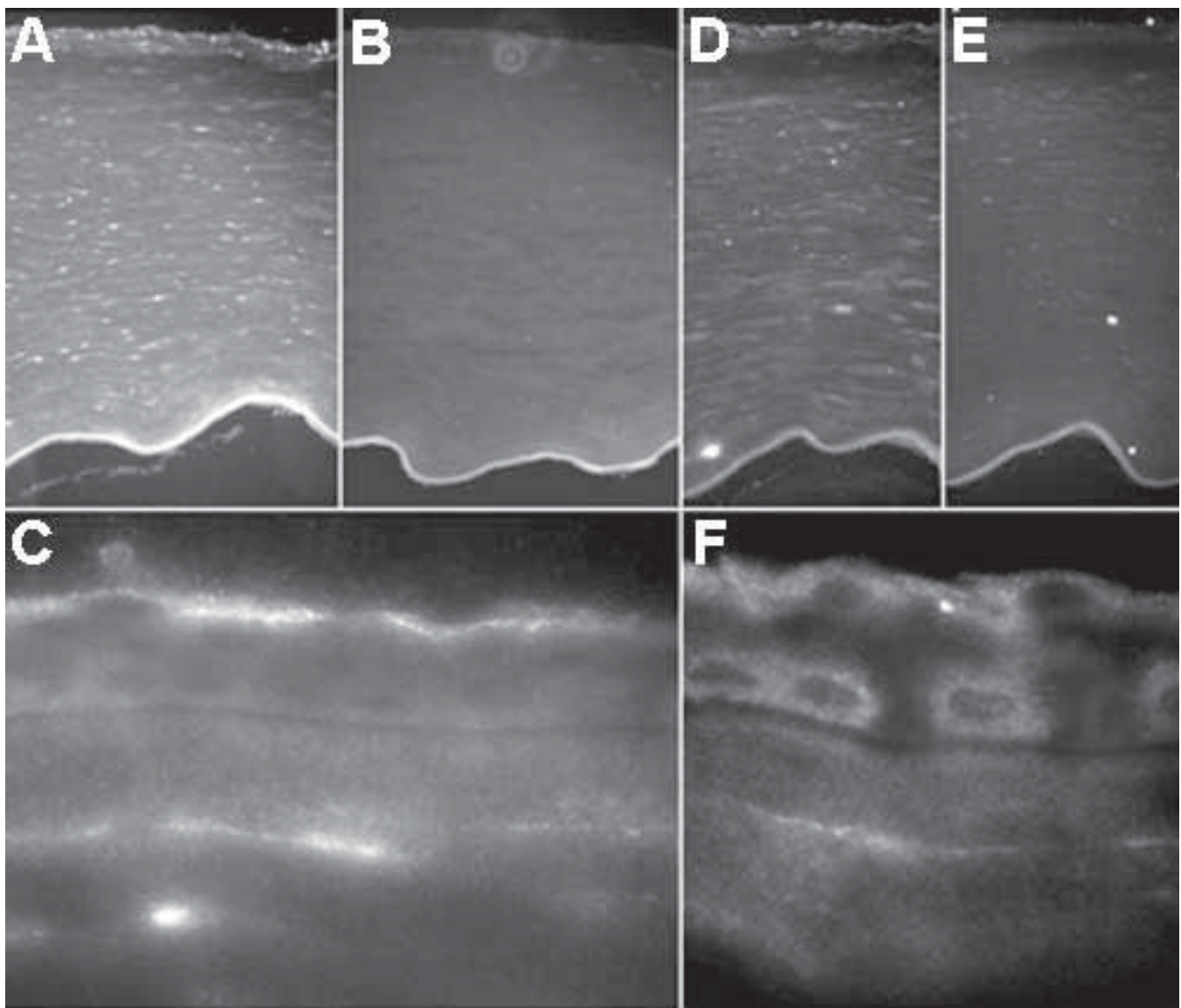


Figure 3. Light microscopic immunofluorescence staining for CIC-2 and CIC-3 in human cornea. **A,D:** Low power view showing labelling of whole cornea. Note that in **A**, the endothelial cell monolayer has become detached from Descemet's layer, while in **D**, the endothelial cell layer is mostly absent. **C,F:** At higher magnification, some regions show pronounced immunolabelling along the apical region of the superficial epithelial cell layer, and in Bowman's layer. Note also the suggestion of intracellular labelling for CIC-3 in certain cells. **B,E:** Pre-absorption control sections, showing absence of specific labelling, except for autofluorescence of Descemet's layer. **A-C:** CIC-2. **D-F:** CIC-3.

expression of a number of additional genes was examined. Cell type specific mRNAs were found to be more widely expressed in the different layers of the cornea than expected (Figure 2, Table 4). This was especially true for the results of gels stained with SYBR gold, (which is about tenfold more sensitive than ethidium bromide) [25]. Indeed, non of the prospective cell type specific genes we studied appeared to be expressed in only a single corneal cell layer. For instance, keratin 12 mRNA was detected in all three layers of the cornea, kidney, muscle, lung, and skin. However, the results obtained did allow us to tentatively conclude that the corneal epithelial

and endothelial cell samples were essentially free from contamination (see Discussion). The positive control genes connexin 43, annexin II, decorin and NBC were present in all 3 corneal layers, as expected (data not shown).

Does the rabbit express CIC-4?: We were unable to obtain PCR products of the expected size for CIC-4 from any of the rabbit tissues tested (cornea, muscle, kidney, lung, and skin) despite designing four sets of PCR primers and using the various primers in combination and in nested reactions. Where products of the incorrect size were generated with CIC-4 primers, these were found to correspond to non-CIC mRNAs when

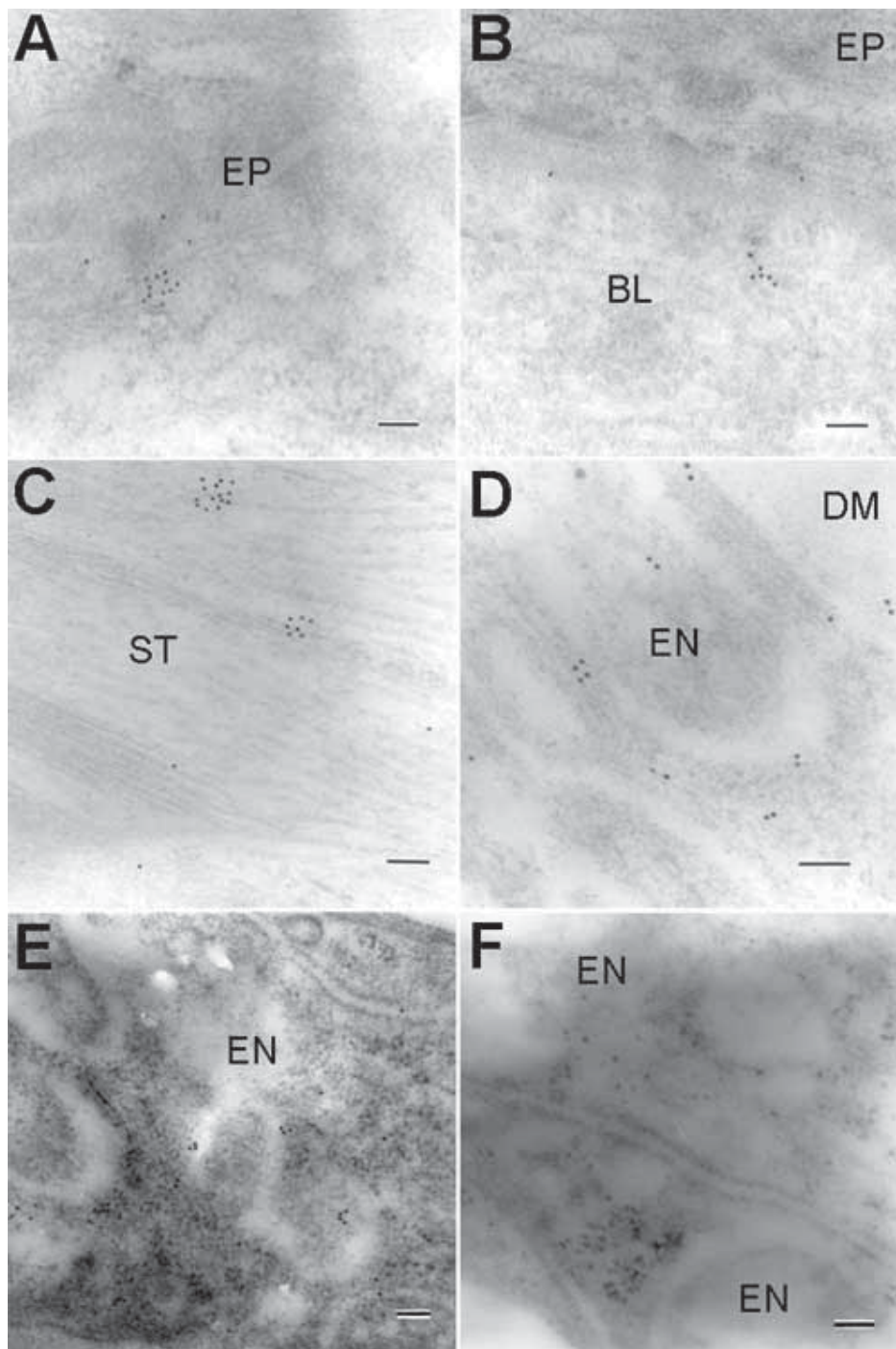


Figure 4. Electron microscopic labelling for CIC-2 in the rat cornea. **A:** Corneal epithelium. **B:** Sub-epithelial stroma. **C:** Middle stroma. **D-F:** Corneal endothelium. Examples of positive labelling are shown in **A-E**. Note that gold particles are localized mostly adjacent to plasma membranes, but also intracellularly. A control section (**F**) is shown for comparison. No gold particles are visible after omission of the primary antibody. The epithelium (EP), Bowman's layer (BL), stroma (ST), endothelium (EN), Descemet's membrane (DM) are labeled. Scale bars represent 100 nm.

sequenced. When tested on mRNA from human kidney, RT-PCR with our original set of CIC-4 primers (Table 1) yielded a strong band of the expected size, which when sequenced, was confirmed as CIC-4. Our results suggest either that (1) the CLCN4 gene, which codes for CIC-4, is not present in the rabbit genome; (2) the rabbit CLCN4 gene's coding region differs markedly from those of human, mouse, and rat (the cDNA sequences from which the rabbit CIC-4 primers were designed); or (3) the rabbit expresses CIC-4 at a level below the detection threshold of RT-PCR in all of the tissues examined.

Immunocytochemical labelling of CIC-2 and CIC-3: Using antibodies raised against CIC subtype specific epitopes in the rat, labelling for CIC-2 and CIC-3 protein was detected in

each layer of the human and rat cornea at the light and electron microscope levels, respectively.

Using immunofluorescence, strong labelling for CIC-2 was seen in stromal keratocytes, in patches of epithelial cells, and in the endothelium (Figure 3A). At higher magnification, a tendency for preferential labelling of the apical region of the superficial epithelial cells was evident (Figure 3C). Labelling for CIC-3 was similar (Figure 3D), although generally it was more diffuse. In addition to the preference for apical labelling in superficial epithelial cells seen with the antibody to CIC-2, it appeared that some cells expressed CIC-3 intracellularly. Pre-absorption control sections in which the respective antigenic peptide was incubated with the primary antibody prior to labelling, showed only autofluorescence of Descemet's

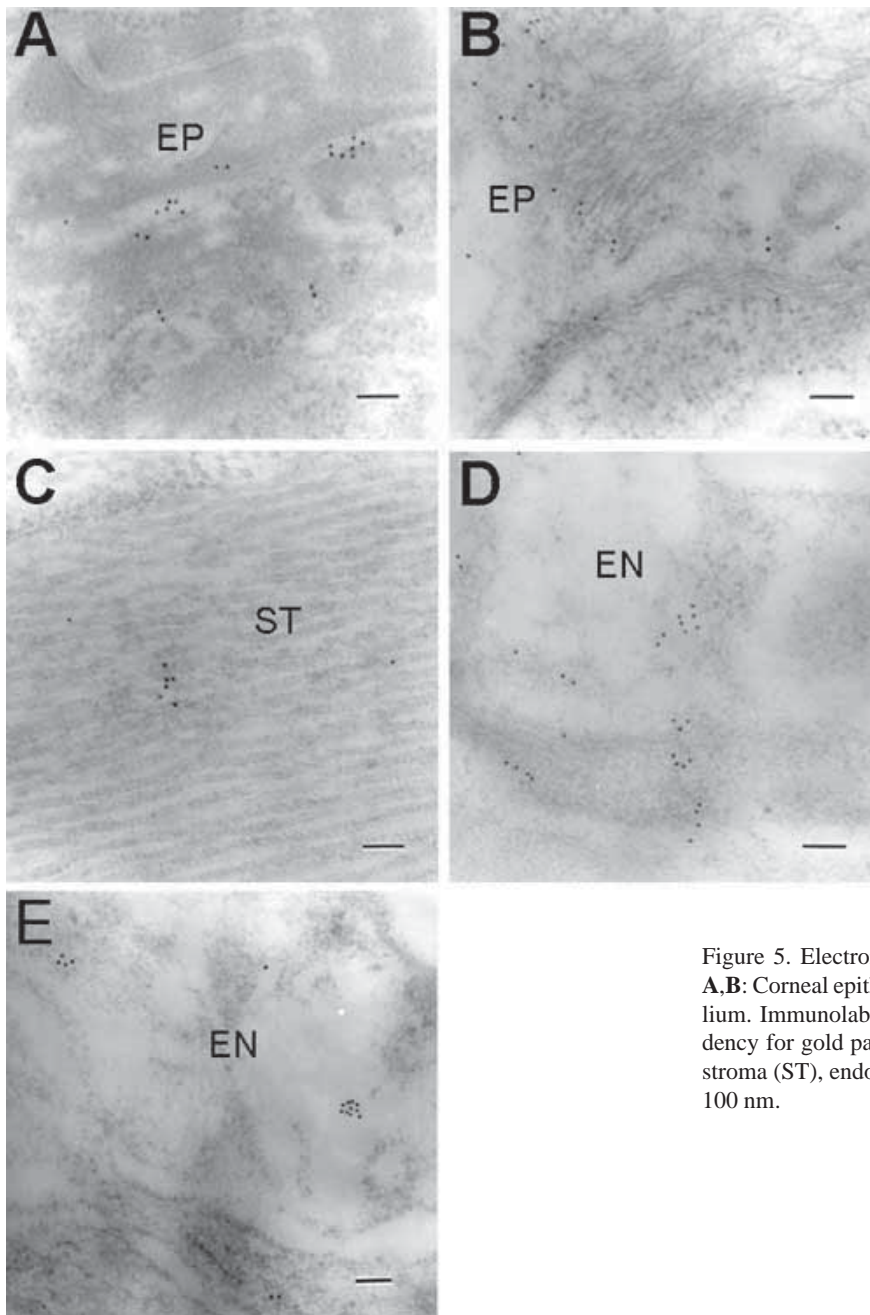


Figure 5. Electron microscopic labelling for CIC-3 in the cornea. **A,B:** Corneal epithelium. **C:** Corneal stroma. **D-E:** Corneal endothelium. Immunolabelling was present in all cell types. Note the tendency for gold particles to appear in clusters. The epithelium (EP), stroma (ST), endothelium (EN) are labeled. All scale bars represent 100 nm.

membrane (Figure 3B,D).

Using immunogold labelling, moderate labelling for CIC-2 was observed in the squamous cell and basal epithelial cells (Figure 4A). Most of the labelling was observed in intercellular spaces or close to the plasma membrane in the peripheral cytoplasm. Labelling was also observed in the sub-epithelial stroma (Figure 4B) and some parts of the middle and posterior stroma (Figure 4C). In addition, there was labelling in the stromal keratocytes near rough endoplasmic reticulum. Most of the labelling in the endothelial cells was in the intercellular spaces and on or close to the lateral membrane (Figure 4D). However, there was also labelling in the endothelial cell cytoplasm (Figure 4D,E). Labelling for CIC-3 was observed in the epithelial cells similar to that for CIC-2. In squamous cells, most of the labelling was in clusters in the intercellular spaces, but was also present in the cytoplasm (Figure 5A). In basal cells, labelling was seen close to cytoplasmic filaments (Figure 5B). Gold particles were also observed in the parts of stroma (Figure 5C), keratocytes, and prominent in the corneal endothelium, again tending to appear in clusters (Figure 5D,E).

DISCUSSION

Comparison with previous studies: Our RT-PCR results show that the mRNAs for CIC-2, CIC-3, CIC-5, CIC-6, and CIC-7 are expressed in the rabbit corneal epithelium and endothelium, and possibly also in the corneal stroma. The skeletal muscle specific CIC-1 and the kidney specific CIC-Ka mRNAs were not detected, consistent with our expectations from studies in other tissues and organs [26-31]. Immunocytochemistry confirmed the expression of CIC-2 and CIC-3 in the human and rat corneal epithelium, endothelium, and stroma. Our results support those of Shepard and Rae [16] who identified a CIC-3 expressed sequence tag (EST) in both rabbit corneal epithelial and endothelial cDNA libraries, and those of Sun et al. [12] who reported CIC-3 mRNA expression in the rabbit corneal endothelium. However, while Sun et al. [12] also found CIC-5 mRNA to be expressed in rabbit corneal endothelium, as we did, they did not detect CIC-2. In a study investigating chloride channel expression in the human corneal epithelium, Itoh et al. [32] found that the mRNAs for CIC-2, CIC-3, CIC-4, CIC-6, and CIC-7 were expressed, while those for CIC-1, CIC-5, and CIC-Ka were not. Thus our finding of CIC-5 mRNA expression in the rabbit corneal epithelium may signify a species difference. It should also be noted that previous studies have clearly demonstrated the presence of mRNA for the cystic fibrosis transmembrane conductance regulator (CFTR) chloride channel in human, rabbit and bovine corneal endothelium [11,12,33,34] and human corneal epithelium [32], and the mRNA for one of the calcium activated chloride channel genes, calcium activated chloride channel-1 (CLCA1; but not that for CLCA2), in human and bovine corneal endothelium [32,35] and human corneal epithelium [32]. Chloride currents have been detected in both normal and wound activated keratocytes, although the molecular basis of these currents have yet to be fully elucidated [36,37].

Cell type specific gene expression: Expression of the keratin 12 gene (KRT12) has been described as corneal epithelial

cell specific [38-42] and, interestingly, mutations in this gene can give rise to a disease manifested only in the cornea: Meesman's corneal dystrophy [41,42]. However, keratin 12 mRNA was found not only in the rabbit corneal epithelium, but also in corneal stroma, corneal endothelium, kidney, lung, muscle and skin (keratin 12 RT-PCR products were sequenced to confirm that the desired target mRNA had been amplified). A species difference again seems the most likely explanation for this result. However, it is also possible that the rabbit KRT12 gene is transcribed in several tissues but only translated in the corneal epithelium.

We reasoned that the wider than expected pattern of mRNA expression of cell type specific genes was most likely due to the high sensitivity of RT-PCR, rather than sample cross-contamination. First, because type VII collagen mRNA could be detected reliably in the corneal epithelium and stroma, but was only detected in 1 of 3 trials in the endothelium, ruling out major contamination of the endothelial cell samples by either of the other two tissue types. Second, collagen types V, VI, and VIII could be detected with ethidium bromide staining in the corneal stroma, but not in the epithelium, ruling out major contamination of the epithelial cell samples by stromal mRNAs. Third, since corneal epithelial cells were collected from eyes that were still intact, endothelial cell contamination of epithelial cell samples would be extremely unlikely. However, contamination of the stromal sample by either corneal epithelial or endothelial cells could not be ruled out with any confidence from our results. Thus we interpret the CIC mRNA expression pattern of the corneal stroma samples with caution. Furthermore, a limitation of our study design was that CIC gene expression and cell type specific gene expression were assessed in different sets of tissue samples. This was done to avoid diluting the corneal endothelial cell sample any further than was absolutely necessary, since we found that such dilution limited the number of CICs that could be detected.

The collection of pure samples of corneal epithelial or endothelial cells by careful scrapping of the cells from their basement membrane can be traced back at least to the work of Kinsey and Cogan [43]. Later, Graymore [44] commented that while the scraping technique was the most accurate method available, constant success in ensuring sample homogeneity could not be guaranteed. Our results suggest that the continued use of the cell scraping technique [12,45] is justified, even for highly sensitive assays such as RT-PCR.

Localization of CIC-2 and CIC-3: Our immunolabelling results suggest a complex distribution pattern for both CIC-2 and CIC-3. The channel proteins appeared to be distributed nonuniformly, with some cells labelling more strongly than others. Moreover, gold particles often appeared in clusters, suggestive of areas of specialized functional compartmentalization. In most cells, gold particles were found intracellularly and adjacent to the plasma membrane. Furthermore, although immunofluorescence microscopy suggested relatively strong labelling of the apical membranes of many superficial epithelial cells, immunogold staining demonstrated labelling of baso-lateral membranes, also. This was also the case for corneal endothelial cells, where neither CIC-2 nor CIC-3 ap-

peared to be restricted to either the apical or baso-lateral membrane.

The role of chloride channels in the cornea: Despite their very different roles in corneal homeostasis, the corneal epithelium and endothelium share the expression of at least 7 different chloride channel mRNAs (CIC-2, CIC-3, CIC-5, CIC-6, CIC-7, CFTR, and CLCA1). This could be interpreted as evidence against a key role for any one particular chloride channel in epithelial or endothelial fluid transport. However, it is of course possible that one or more of these chloride channels play an essential role in the endothelium, and yet serve a minor or different function in the epithelium. A high level of gene expression may be indicative of such a role [32] but again, this theory is not well supported in practice, as different channels may exhibit considerable differences in their gating properties, mRNA translational efficiency, protein half life, and membrane turnover [7,46]. As future, fundamental, studies reach a consensus regarding the functional properties and precise subcellular distributions of each member of the CIC family [17,18,47-49] the likely roles of these channels in the cornea should become clearer.

In terms of transendothelial ion transport in the cornea, plasma membrane bound chloride channels may allow the dissipation of intracellular chloride loaded into cells by $\text{Na}^+\text{K}^+2\text{Cl}^-$ cotransport and/or $\text{HCO}_3^-/\text{Cl}^-$ exchange across the basolateral membrane [50]. For CIC-2 and CIC-3 channels located on the basolateral membrane, chloride transport would not contribute to the transendothelial ion flux: Instead chloride would simply be recycled. However, for channels located on the apical membrane there would be a route for chloride transport across the endothelium that would contribute directly to corneal deturgescence. Such a system of coupled basolateral $\text{Na}^+\text{K}^+2\text{Cl}^-$ cotransport and apical chloride channel efflux is found in intestinal crypt cells [51].

Anion channels on the apical membrane of the corneal endothelium could serve as an exit route for HCO_3^- ions loaded intracellularly by basolateral $\text{Na}^+2\text{HCO}_3^-$ cotransport (via NBC), carbonic anhydrase IV, and/or $\text{HCO}_3^-/\text{Cl}^-$ exchange. Here again, the transendothelial HCO_3^- flux generated would contribute to corneal deturgescence. If HCO_3^- is the dominant ion that is actively transported across the cornea, then it seems likely that an as yet unknown system of tailoring the selectivity of apical located chloride channels for HCO_3^- over Cl^- must be in place to enable the preferential dissipation of HCO_3^- , or that a novel bicarbonate selective anion channel exists. Evidence is lacking for both of these options, although it is interesting to note that Reddy and Quinton [52] have recently shown that the selectivity of CFTR for Cl^- compared to HCO_3^- can be modulated by glutamate and ATP, respectively.

ACKNOWLEDGEMENTS

This work was supported in part by NEI grant EY00160 from the National Institute of Health.

REFERENCES

- Maurice DM. The cornea and sclera. In: Davson H, editor. The eye. Orlando: Academic Press; 1984. pp. 1-158.

- Fischbarg J, Maurice DM. An update on corneal hydration control. *Exp Eye Res* 2004; 78:537-41.
- Hodson SA. Corneal stromal swelling. *Prog Retin Eye Res* 1997; 16:99-116.
- Bonanno JA. Identity and regulation of ion transport mechanisms in the corneal endothelium. *Prog Retin Eye Res* 2003; 22:69-94.
- Kostyuk O, Nalovina O, Mubard TM, Regini JW, Meek KM, Quantock AJ, Elliott GF, Hodson SA. Transparency of the bovine corneal stroma at physiological hydration and its dependence on concentration of the ambient anion. *J Physiol* 2002; 543:633-42.
- Ashcroft FM. Ion channels and disease. San Diego: Academic Press; 2000.
- Jentsch TJ. Diverse roles of CLC chloride channels: lessons from disease in mice and man. *J Physiol* 2002; 544:S8-S9.
- Hodson S, Miller F. The bicarbonate ion pump in the endothelium which regulates the hydration of rabbit cornea. *J Physiol* 1976; 263:563-77.
- Huff JW, Green K. Characteristics of bicarbonate, sodium, and chloride fluxes in the rabbit corneal endothelium. *Exp Eye Res* 1983; 36:607-15.
- Winkler BS, Riley MV, Peters MI, Williams FJ. Chloride is required for fluid transport by the rabbit corneal endothelium. *Am J Physiol* 1992; 262:C1167-74.
- Sun XC, Bonanno JA. Expression, localization, and functional evaluation of CFTR in bovine corneal endothelial cells. *Am J Physiol Cell Physiol* 2002; 282:C673-83.
- Sun XC, McCutcheon C, Bertram P, Xie Q, Bonanno JA. Studies on the expression of mRNA for anion transport related proteins in corneal endothelial cells. *Curr Eye Res* 2001; 22:1-7.
- Srinivas SP, Bonanno JA. Swelling activated chloride channels in corneal endothelium. *Invest Ophthalmol Vis Sci* 1996; 37:S672.
- Srinivas SP, Bonanno JA, Hughes BA. Assessment of swelling-activated Cl^- channels using the halide-sensitive fluorescent indicator 6-methoxy-N-(3-sulfopropyl)quinolinium. *Biophys J* 1998; 75:115-23.
- Srinivas SP, Guan Y, Bonanno JA. Swelling activated chloride channels in cultured bovine corneal endothelial cells. *Exp Eye Res* 1999; 68:165-77.
- Shepard AR, Rae JL. Ion transporters and receptors in cDNA libraries from lens and cornea epithelia. *Curr Eye Res* 1998; 17:708-19.
- Roman RM, Smith RL, Feranchak AP, Clayton GH, Doctor RB, Fitz JG. CIC-2 chloride channels contribute to HTC cell volume homeostasis. *Am J Physiol Gastrointest Liver Physiol* 2001; 280:G344-53.
- Weylandt KH, Valverde MA, Nobles M, Raguz S, Amey JS, Diaz M, Nastrucci C, Higgins CF, Sardini A. Human CIC-3 is not the swelling-activated chloride channel involved in cell volume regulation. *J Biol Chem* 2001; 276:17461-7.
- Davies N, Guggenheim JA, Wigham CG. PCR-based investigations of chloride channels in rabbit corneal endothelium. *Invest Ophthalmol Vis Sci* 2001; 42:S275.
- Frost MR, Guggenheim JA. Mammalian polyadenylation sites: implications for differential display. *Nucleic Acids Res* 1999; 27:1386-91.
- Thompson JD, Higgins DG, Gibson TJ. CLUSTAL W: improving the sensitivity of progressive multiple sequence alignment through sequence weighting, position-specific gap penalties and weight matrix choice. *Nucleic Acids Res* 1994; 22:4673-80.
- Breslauer KJ, Frank R, Blocker H, Marky LA. Predicting DNA

- duplex stability from the base sequence. *Proc Natl Acad Sci U S A* 1986; 83:3746-50.
23. Inoue H, Nojima H, Okayama H. High efficiency transformation of *Escherichia coli* with plasmids. *Gene* 1990; 96:23-8.
 24. Britton FC, Hatton WJ, Rossow CF, Duan D, Hume JR, Horowitz B. Molecular distribution of volume-regulated chloride channels (CIC-2 and CIC-3) in cardiac tissues. *Am J Physiol Heart Circ Physiol* 2000; 279:H2225-33.
 25. Tuma RS, Beaudet MP, Jin X, Jones LJ, Cheung CY, Yue S, Singer VL. Characterization of SYBR Gold nucleic acid gel stain: a dye optimized for use with 300-nm ultraviolet transilluminators. *Anal Biochem* 1999; 268:278-88.
 26. Steinmeyer K, Schwappach B, Bens M, Vandewalle A, Jentsch TJ. Cloning and functional expression of rat CLC-5, a chloride channel related to kidney disease. *J Biol Chem* 1995; 270:31172-7.
 27. Kieferle S, Fong P, Bens M, Vandewalle A, Jentsch TJ. Two highly homologous members of the CIC chloride channel family in both rat and human kidney. *Proc Natl Acad Sci U S A* 1994; 91:6943-7.
 28. Adachi S, Uchida S, Ito H, Hata M, Hiroe M, Marumo F, Sasaki S. Two isoforms of a chloride channel predominantly expressed in thick ascending limb of Henle's loop and collecting ducts of rat kidney. *J Biol Chem* 1994; 269:17677-83.
 29. Uchida S, Sasaki S, Furukawa T, Hiraoka M, Imai T, Hirata Y, Marumo F. Molecular cloning of a chloride channel that is regulated by dehydration and expressed predominantly in kidney medulla. *J Biol Chem* 1993; 268:3821-4. Erratum in: *J Biol Chem* 1994; 269:19192.
 30. Koch MC, Steinmeyer K, Lorenz C, Ricker K, Wolf F, Otto M, Zoll B, Lehmann-Horn F, Grzeschik KH, Jentsch TJ. The skeletal muscle chloride channel in dominant and recessive human myotonia. *Science* 1992; 257:797-800.
 31. Steinmeyer K, Ortland C, Jentsch TJ. Primary structure and functional expression of a developmentally regulated skeletal muscle chloride channel. *Nature* 1991; 354:301-4.
 32. Itoh R, Kawamoto S, Miyamoto Y, Kinoshita S, Okubo K. Isolation and characterization of a Ca(2+)-activated chloride channel from human corneal epithelium. *Curr Eye Res* 2000; 21:918-25.
 33. Al-Nakkash L, Reinach PS. Activation of a CFTR-mediated chloride current in a rabbit corneal epithelial cell line. *Invest Ophthalmol Vis Sci* 2001; 42:2364-70.
 34. Sun XC, Zhai CB, Cui M, Chen Y, Levin LR, Buck J, Bonanno JA. HCO(3)(-)-dependent soluble adenylyl cyclase activates cystic fibrosis transmembrane conductance regulator in corneal endothelium. *Am J Physiol Cell Physiol* 2003; 284:C1114-22.
 35. Zhang Y, Xie Q, Sun XC, Bonanno JA. Enhancement of HCO(3)(-) permeability across the apical membrane of bovine corneal endothelium by multiple signaling pathways. *Invest Ophthalmol Vis Sci* 2002; 43:1146-53.
 36. Watsky MA, Wang J. G-protein involvement in the phospholipid growth factor-mediated activation of a Cl- current in corneal keratocytes. *ARVO Annual Meeting*; 2003 May 4-9; Fort Lauderdale (FL).
 37. Watsky MA. Lysophosphatidic acid, serum, and hyposmolarity activate Cl- currents in corneal keratocytes. *Am J Physiol* 1995; 269:C1385-93.
 38. Wang JJ, Carlson EC, Liu CY, Kao CW, Hu FR, Kao WW. Cis-regulatory elements of the mouse Krt1.12 gene. *Mol Vis* 2002; 8:94-101.
 39. Liu JJ, Kao WW, Wilson SE. Corneal epithelium-specific mouse keratin K12 promoter. *Exp Eye Res* 1999; 68:295-301.
 40. Shiraishi A, Converse RL, Liu CY, Zhou F, Kao CW, Kao WW. Identification of the cornea-specific keratin 12 promoter by in vivo particle-mediated gene transfer. *Invest Ophthalmol Vis Sci* 1998; 39:2554-61.
 41. Nishida K, Honma Y, Dota A, Kawasaki S, Adachi W, Nakamura T, Quantock AJ, Hosotani H, Yamamoto S, Okada M, Shimomura Y, Kinoshita S. Isolation and chromosomal localization of a cornea-specific human keratin 12 gene and detection of four mutations in Meesmann corneal epithelial dystrophy. *Am J Hum Genet* 1997; 61:1268-75.
 42. Irvine AD, Corden LD, Swensson O, Swensson B, Moore JE, Frazer DG, Smith FJ, Knowlton RG, Christophers E, Rochels R, Uitto J, McLean WH. Mutations in cornea-specific keratin K3 or K12 genes cause Meesmann's corneal dystrophy. *Nat Genet* 1997; 16:184-7.
 43. Kinsey VE, Cogan DG. The cornea. IV. Hydration, properties of the whole cornea. *Arch Ophthalmol* 1942; 28:449-463.
 44. Graymore CN. Lactic acid dehydrogenase (LDH) in the cornea. II. The effect of pyruvate concentration on the rate of reaction. *Exp Eye Res* 1966; 5:325-8.
 45. Riley MV, Winkler BS, Starnes CA, Peters MI. Adenosine promotes regulation of corneal hydration through cyclic adenosine monophosphate. *Invest Ophthalmol Vis Sci* 1996; 37:1-10.
 46. Jentsch TJ, Gunther W, Pusch M, Schwappach B. Properties of voltage-gated chloride channels of the CIC gene family. *J Physiol* 1995; 482:19S-25S.
 47. Lipecka J, Bali M, Thomas A, Fanen P, Edelman A, Fritsch J. Distribution of CIC-2 chloride channel in rat and human epithelial tissues. *Am J Physiol Cell Physiol* 2002; 282:C805-16.
 48. Huang P, Liu J, Di A, Robinson NC, Musch MW, Kaetzel MA, Nelson DJ. Regulation of human CLC-3 channels by multifunctional Ca2+/calmodulin-dependent protein kinase. *J Biol Chem* 2001; 276:20093-100.
 49. Murray CB, Morales MM, Flotte TR, McGrath-Morrow SA, Guggino WB, Zeitlin PL. CIC-2: a developmentally dependent chloride channel expressed in the fetal lung and downregulated after birth. *Am J Respir Cell Mol Biol* 1995; 12:597-604.
 50. Jelamskii S, Sun XC, Herse P, Bonanno JA. Basolateral Na(+)-K(+)-2Cl(-) cotransport in cultured and fresh bovine corneal endothelium. *Invest Ophthalmol Vis Sci* 2000; 41:488-95.
 51. Jentsch TJ, Stein V, Weinreich F, Zdebek AA. Molecular structure and physiological function of chloride channels. *Physiol Rev* 2002; 82:503-68. Erratum in: *Physiol Rev* 2003; 83:following table of contents.
 52. Reddy MM, Quinton PM. Control of dynamic CFTR selectivity by glutamate and ATP in epithelial cells. *Nature* 2003; 423:756-60.